Atmos. Chem. Phys. Discuss., 7, 4481–4519, 2007
www.atmos-chem-phys-discuss.net/7/4481/2007/

Atmospheric Chemistry and Physics Discussions

Remote sensing the vertical profile of cloud droplet effective radius, thermodynamic phase, and temperature

J. Vanderlei Martins[1,2], A. Marshak[2], L. A. Remer[2], D. Rosenfeld[3], Y. J. Kaufman[2], R. Fernandez-Borda[4], I. Koren[5], V. Zubko[6], and P. Artaxo[7]

[1]Department of Physics, and Joint Center for Earth Systems Technology, University of Maryland Baltimore County, Baltimore, MD, USA
[2]Climate and Radiation Branch, NASA – Goddard Space Flight Center, Greenbelt, MD, USA
[3]Institute of Earth Sciences, The Hebrew University of Jerusalem, Israel
[4]Catholic University, Washington DC, USA
[5]Department of Environmental Sciences, Weizmann Institute, Rehovot, Israel
[6]Advanced Computation Technologies, Inc., Lanham, MD, USA
[7]Institute of Physics, University of Sao Paulo, Brazil

Received: 7 November 2006 – Accepted: 30 January 2007 – Published: 30 March 2007

Correspondence to: J. Vanderlei Martins (martins@climate.gsfc.nasa.gov)

Abstract

Cloud-aerosol interaction is no longer simply a radiative problem, but one affecting the water cycle, the weather, and the total energy balance including the spatial and temporal distribution of latent heat release. Information on the vertical distribution of cloud droplet microphysics and thermodynamic phase as a function of temperature or height, can be correlated with details of the aerosol field to provide insight on how these particles are affecting cloud properties and its consequences to cloud lifetime, precipitation, water cycle, and general energy balance. Unfortunately, today's experimental methods still lack the observational tools that can characterize the true evolution of the cloud microphysical, spatial and temporal structure in the cloud droplet scale, and then link these characteristics to environmental factors and properties of the cloud condensation nuclei.

Here we propose and demonstrate a new experimental approach (the cloud scanner instrument) that provides the microphysical information missed in current experiments and remote sensing options. Cloud scanner measurements can be performed from aircraft, ground, or satellite by scanning the side of the clouds from the base to the top, providing us with the unique opportunity of obtaining snapshots of the cloud droplet microphysical and thermodynamic states as a function of height and brightness temperature in clouds at several development stages. The brightness temperature profile of the cloud side can be directly associated with the thermodynamic phase of the droplets to provide information on the glaciation temperature as a function of different ambient conditions, aerosol concentration, and type. An aircraft prototype of the cloud scanner was built and flew in a field campaign in Brazil.

The CLAIM-3D (3-Dimensional Cloud Aerosol Interaction Mission) satellite concept proposed here combines several techniques to simultaneously measure the vertical profile of cloud microphysics, thermodynamic phase, brightness temperature, and aerosol amount and type in the neighborhood of the clouds. The wide wavelength range, and the use of mutli-angle polarization measurements proposed for this mis-

sion allow us to estimate the availability and characteristics of aerosol particles acting as cloud condensation nuclei, and their effects on the cloud microphysical structure. These results can provide unprecedented details on the response of cloud droplet microphysics to natural and anthropogenic aerosols in the size scale where the interaction really happens.

1 Introduction

Clouds and precipitation play a crucial role in the Earth's energy balance and water cycle. In addition, clouds and the release of latent heat during precipitation provide much of the energy that drives the circulation, especially the tropical circulation. Thus, to understand atmospheric dynamics we need to understand cloud development and the factors that influence precipitation in cloud systems. Clouds are highly dynamic systems, strongly controlled by environmental parameters and by the presence, concentration and characteristics of cloud condensation nuclei (aerosol particles). Most cloud droplets are seeded and strongly influenced by cloud condensation nuclei (CCN) aerosols. To understand clouds and precipitation at the microphysical level we must understand cloud-aerosol interaction at this level. A landmark in our understanding of aerosol-cloud interaction was the Twomey's theory (1977) in which he explained that high concentrations of aerosols can reduce the effective droplet size and increase cloud albedo for a constant amount of liquid water. Albrecht et al. (1989) expanded this theory by explaining that high aerosol concentrations can also narrow the droplet size distribution, suppressing precipitation and prolonging cloud lifetime of marine stratocumulus. Rosenfeld et al. (2006a) showed that the feedback through precipitation greatly enhances the sensitivity of the cloud cover and dynamic regime to small differences in aerosol concentrations. Cloud-aerosol interactions dominate not only the dynamics of marine shallow clouds, but also the lifetime and the vertical disposition of latent heat of deep convective clouds over ocean and even more strongly over land. Rosenfeld (2006) shows from observational data (Andreae et al., 2004; Williams et al., 2002)

and simulation (Khain et al., 2005) studies that aerosol-induced changes of cloud microstructure have profound impact on the precipitation, dynamic evolution and vertical disposition of latent heat release.

Aerosols affect clouds also by their radiative properties. Hansen et al. (1997) that absorbing aerosol can effectively decrease cloud lifetime by heating the cloud layers. Ackerman et al. (2000) modeled this situation and Koren et al. (2004) observed quantitatively the inhibition of certain types of clouds in the Amazon due to the presence of heavy smoke. Recently, Kaufman and Koren (2006) analyzing AERONET data (Holben et al., 1998) found that absorbing and non-absorbing aerosols affect cloud cover differently: while absorbing aerosols prevent clouds from forming, non-absorbing aerosols enhance cloud cover by suppressing precipitation.

All of these cloud-aerosol interaction theories and studies have one thing in common. They are all focused on how cloud-aerosol interaction affects the earth's radiation budget. One of the reasons for this focus is the emphasis given by the climate community, who cites the IPCC (Intergovernmental Panel on Climate Change) reported uncertainty in radiative forcing estimates due to the uncertainty introduced by cloud-aerosol interaction. In parallel, new dimensions to cloud-aerosol interaction (summarized in Rosenfeld, 2006a) has been introduced by Rosenfeld and Lensky (1998), Rosenfeld (1999, 2000), Rosenfeld and Woodley (2003), Rosenfeld and Ulbrich (2003) and Andreae et al. (2004), emphasizing the aerosol effect on the cloud microphysics and precipitation. Also, another component of the energy budget driven by latent heating release was recently proposed by Rosenfeld (2006). This new focus claims that cloud-aerosol interaction is no longer simply a radiative problem, but one affecting the water cycle, the weather, and the total energy balance including the spatial and temporal distribution of latent heat release. In particular, Andreae et al. (2004 – see Fig. 1) showed how the vertical profile of effective radius changed as a function of the amount of biomass burning aerosols using in situ measurements.

Although several basic processes explaining cloud formation and evolution are well established, there are many unresolved fundamental issues concerning the under-

standing of real clouds and their temporal and spatial evolution. The explanation of some of these issues, like the lack of fundamental understanding of the glaciation of clouds, or the warm rain paradox, are being targeted by the scientific community for long time (e.g. McGraw and Liu, 2003). To alleviate some of this uncertainty several field campaigns have been performed to study developing convective systems (CRYSTAL-FACE, CAMEX, SMOCC, others). However, these experiments lacked the experimental observations that could characterize the true evolution of the cloud microphysics spatial and temporal structure, and then link these development characteristics to environmental factors and available CCN.

Traditionally, our understanding of the changing vertical structure of a developing cloud was mostly based on radar and in situ measurements collected by aircraft. Precipitation radars tell us about the vertical development of precipitation sized droplets in clouds and gives information on the thermodynamic phase of the hydrometeors. Millimeter wavelength cloud radars (Clothiaux et al., 1999) determine cloud boundaries (cloud bottoms and tops). Though they also provide vertical velocities of cloud constituent, they have very limited capability (e.g., Fricsh et al., 1995) of measuring vertical profiles of small droplets. Radars alone cannot tell us a complete microphysical story because they miss the characterization of the smaller-sized cloud droplets where the story begins. In situ measurements can measure cloud droplets, but they are very limited in terms of characterizing the vertical structure of clouds. In many cases, the time an aircraft would take to climb from cloud base to cloud top measuring its physical properties is enough for the cloud to form, evolve and dissipate. In many cases there is also the danger of flying inside highly convective systems and there are often altitude limitations for most of the available research aircraft.

Recently satellite remote sensing measurements have provided information that has led to the revolutionary re-thinking of our perceptions of cloud-aerosol interaction (Rosenfeld and Lensky, 1998). Satellites can provide insight and an impressive statistical data-base of cloud microphysics at cloud top, coupled to column aerosol properties surrounding the cloud. However, all these satellite inferences have been based on 1 to

2 km resolution single snap shot imagery of the cloud tops, or large statistics on 1x1dg resolution MODIS data (Kaufman et al., 2005, Koren et al., 2005). The satellite-derived vertical evolution is a result of composition of many cloud pixels at different degrees of evolution, assuming that the ensemble represents the evolution of a single cloud with height and time (Freud et al., 2005). Additional support for this assumption was obtained from rapid scan of geostationary microphysical images tracking the evolution of individual clouds (Lensky and Rosenfeld, 2006), but with the poor spatial resolution that can be obtained from a geostationary orbit. While this method of inferring vertical evolution is useful, it relies on strong assumptions and poses many limitations.

Despite of all the physics we learned from in situ measurements in the clouds and from the large remote sensing statistics, there is still a big gap to be filled. We must add large statistics with detailed information about the cloud vertical structure on a cloud by cloud basis. We are after a deep understanding of the processes driving the effect of aerosol on clouds. We need a methodology that at the same time will provide:

- a snapshot with similar or better level of details than in situ measurements of the vertical structure of cloud microphysics can provide.

- large enough statistics that would allow us to make confident conclusions about the physical processes inside the cloud

These two conditions cannot be met today by either remote sensing or in situ capabilities. Each in situ cloud measurement, takes at least tens of minutes of the cloud lifetime which allow many changes in the cloud structure. The collection of data showed by Andreae et al. (2004) and in Fig. 8 of Rosenfeld et al. (2006b) took more than one experiment, in different countries, and different years to collect enough data for their conclusions. Also, in situ aircraft cannot penetrate the strongest thunderstorms.

Here, we demonstrate a new approach that provides the information missed in experiments and in today's remote sensing options: the details of vertical, horizontal and temporal development of cloud microphysical structure in a developing cloud. We will use new measurements of cloud microphysics in conjunction with other measurements of cloud and aerosol characteristics to improve our understanding of the factors influ-

encing cloud development, and the onset and character of precipitation.

In order to perform these measurements a new aircraft instrument (the cloud scanner system) was developed and built to observe cloud side radiances from the ultraviolet to the thermal infrared. The current model of the cloud scanner consists of a scanning spectrometer system with a 1dg instantaneous field of view, 120 dg total scanning capability, 1nm spectral resolution from 350–2500 nm, and one thermal infrared band centered at 11 μm. The first results from the cloud scanner measurements in tropical clouds over Brazil will be presented in Sect. 3 of this paper.

1.1 Effect of aerosol on cloud microphysics, thermodynamics, and precipitation

Figure 1 illustrates the changes we might observe in a cloud as more and more CCN become available. The figure is based on the conceptual models of Rosenfeld and Lensky (1998) and Rosenfeld and Woodley (2003), which were later confirmed by the modeling work of Khain et al. (2001) and by the observations presented in Fig. 5 of Andreae et al. (2004). The plot shows the effective radius of cloud particles, both water droplets and ice particles, as a function of temperature in a cloud. The temperature is plotted on the vertical axis because it is strongly dependent on altitude and thus used as a proxy for height in the cloud.

The cleanest cloud, the one with the least number of CCN is represented by the lightest gray profile. Travelling upwards from the base of this clean cloud provides immediately a regime of collision-coalescence where liquid droplets quickly grow to larger sizes with the cloud updraft. Here there is the largest increase of r_{eff} with height (Region C in Fig. 1). At relatively low altitude the cloud droplets are large enough to begin falling as warm rain (Region R in Fig. 1), and the droplet growth slows. If the updraft continues, the water droplets begin to freeze at a relatively low altitude, entering a second growth region where ice is forming in a mixed phase regime (Region M in Fig. 1). Soon all the particles are ice and the glaciated region begins (Region G in Fig. 1).

By contrast, the heavily polluted case with an overabundance of CCN is denoted by

the curve with black line. Here, at cloud base, the cloud water has been divided into many more but smaller cloud droplets than in the gray curves (Twomey, 1977). The cloud droplets start at smaller sizes and they remain smaller as we follow the updraft to colder temperatures. The smaller droplets are too small to collide and coalesce and they grow by diffusion processes only (Region D in Fig. 1). Diffusional growth is much slower. The droplets never reach liquid precipitation sizes and begin to freeze only at much colder temperatures, reaching the mixed phase region and glaciation levels much higher in the cloud. At the extreme liquid cloud drops can reach the homogeneous freezing isotherm of –38°C, as observed by in situ measurements of continental convective clouds (Rosenfeld and Woodley, 2000; Rosenfeld et al., 2006b). The medium gray profile shows a case with a moderate amount of CCN.

The cloud responds to increases of available CCN by suppressing collision-coalescence due to the more numerous and relatively smaller droplets and narrower size distribution widths, and the delay on the water droplet freezing allowing in some case the supercooled water to exist closer to temperatures of homogeneous freezing of water vapor molecules (–38°C). Khain et al. (2001) pointed out that the probability of immersion freezing of small droplets with radii below 10 μm is negligibly small, as well as the effect of contact freezing. Heterogeneous freezing is just not efficient in these cases. The collision efficiencies between ice crystals with size below 100 μm and small droplets are close to zero. Cotton (2005) noticed that there are two theories describing the nucleation of a cloud droplet or raindrop by an ice nucleus, which is immersed within the drop (the immersion-freezing). One stochastic theory saying that at a given degree of supercooling not all droplets will freeze at the same time, and a second – called singular theory – holding that at a given degree of supercooling, the probability of freezing depends solely on the likelihood that the droplet contains an active freezing nuclei. Both theories predict that the probability of freezing increases exponentially with the degree of supercooling and with the volume (or size) of the droplet. Thus for small cloud droplets at small degrees of supercooling, this mechanism of nucleation is not effective, re-affirming the delay in droplet freezing following the smaller cloud droplets

caused by high concentration of pollution aerosols.

This delay of the glaciation process is an additional feedback and strong aerosol-cloud interaction effect that further delays the droplet growth and the onset of precipitation. Suppressing rainout will bring additional supercooled water aloft, and so release more latent heat of freezing (Rosenfeld, 2006a). Lohmann (2002) also discussed the effect of soot particles on glaciation, and on the lifetime of ice and mixed phase clouds. Although this paper was focused on the radiative cloud-mediated effect of soot aerosols, the same processes affect the cloud lifetime and precipitation. Her results indicate that soot particles, acting as ice nuclei, can significantly change the efficiency of droplet freezing and contribute to modulate the droplet growth and the onset of precipitation in convective clouds.

Thus there are two measurable cloud responses to increasing CCN in a cloud: (1) the change in cloud effective radius profiles and (2) the change in altitude of the glaciation level. Our proposed remote sensing method is able to resolve both of these responses.

2 Measurements of the cloud side radiances and its information content

2.1 Traditional passive remote sensing of cloud top properties

Traditional remote sensing of cloud microphysical properties assumes that satellites observe only cloud tops, and that clouds behave like infinite plane parallel objects. The solar spectrum reflected by clouds and measured by satellites or from the ground has been long used to measure cloud microphysical and thermodynamic properties. Nakajima and King (1990), and Nakajima et al. (1991) established a two parameter diagram (hereafter called in this paper by Nakajima-King diagram) that converts cloud reflected radiances in two wavelengths (one non-absorbing, usually 0.66 or 0.87 μm, and one absorbing, usually 1.6, 2.1, or 3.7 μm) into two physical parameters of the cloud: effective radius at the upper part of the cloud, and the total cloud optical depth. The cloud reflectance in the absorbing wavelength is mainly sensitive to the droplet

effective radius while the cloud reflectance in the non-absorbing wavelength is more sensitive to the cloud optical depth. Based on the spectral dependence differences between the refractive indices of water and ice, Platnick et al. (2003) review several algorithms used for the measurement of cloud top properties by MODIS, including effective radius, thermodynamic phase, and cloud top pressure.

As proposed by Rosenfeld and Lensky (1998), and further applied in large statistics of convective clouds by Koren et al. (2005), and on shallower clouds by Kaufman et al. (2005), the satellite remote sensing of cloud top properties in a large cloud field containing numerous clouds of different heights have provided important information on the aerosol effect on the vertical profile of the droplet effective radius. The main assumption in this approach is that a cloud top at a given altitude (and/or a given temperature) represents the same state as a point at the same altitude, inside a higher cloud (Freud et al., 2005). Another important assumption here is that the whole cloud field, which in some cases may represent hundreds of kilometers, is homogeneously subjected to the same meteorological and aerosol conditions.

Following these important results, the main motivation for the current work was to develop a methodology to provide the vertical profile of cloud droplet sizes, and thermodynamic phase without the above strong assumptions of the cloud top remote sensing approach, and with better statistics and temporal resolution than those provided by in situ measurements.

2.2 What can we learn by observing the cloud sides

Equivalently to cloud tops, solar radiation photons reflected by the side of the clouds also carry information about the microphysical and thermodynamical properties of cloud droplets. Similarly to the cloud top case, the absorption properties of water and ice particles inside the clouds is inversely related to the droplet effective radius, and analogues to the Nakajima-King type of diagrams can also be constructed for this particular geometry. Furthermore, the cloud side radiances have the additional advantage of carrying information about the vertical position in the cloud profile, allowing for

the vertical profiling of cloud droplet sizes and thermodynamic phase. As discussed previously, this vertical profile is very sensitive to the aerosol conditions imposed to the cloud field. Therefore, cloud side measurements provide us with the unique opportunity of obtaining snapshots of the cloud droplet microphysical and thermodynamic states as a function of height and brightness temperature. The brightness temperature profile of the cloud side can be directly associated with the thermodynamic phase of the droplets to provide information on the glaciation temperature of the droplets as a function of different ambient conditions, aerosol concentration, and type. The different penetration of near infrared wavelengths into the cloud (Platnick , 2000, and 2001, Chang and Li, 2002 and 2003), can also be used from the cloud side to help verifying the constancy of the effective radius at a given altitude. In general, measurements from the cloud side can provide essential information about the evolution of cloud microphysical processes and the important steps that droplets and ice particles undergo before the onset of precipitation.

The combination of these key elements can provide unprecedented information to help our understanding of the effect of aerosols on cloud microphysics and precipitation. These measurements can be done from aircraft, ground, or satellite by scanning the side of the clouds from the base to the top measuring the radiance in selected wavelengths suitable for the retrieval of effective radius, temperature, and the thermodynamic phase. Cloud side measurements have been utilized before from the ground, for the separation between cloud droplet ice and water phases (Pilewski et al., 1987a and b), but, to our knowledge, this is the first time that this approach is being applied to retrieve the vertical profile of cloud droplet size, as a function of phase, and brightness temperature.

2.3 Ground based and aircraft observation geometry of cloud sides

Cloud side observations can be performed from the ground, from mountain tops, aircraft or from satellites with specific advantages and disadvantages on each case. The main disadvantage of the ground-based observations is the relatively thick atmospheric

column observed between the instrument and the cloud mainly at water vapor absorption channels and, in particular, in thermal wavelengths where the combination between high temperatures near the surface and the high water vapor emissivity produce large background noise over the lower temperature for the cloud of interest. Another disadvantage of observations from the ground is the prevalence of cloud shadows due to relatively large scattering angles. Observations from low altitude aircraft and mountain tops eliminate most of the problems with water vapor absorption, temperature and its IR emissivity. Figure 2 show a schematic diagram of low altitude aircraft observations of deep convective clouds using a side scanning geometry. In this case, the aircraft flies on the side of convective clouds and measures the cloud from the base to the top in several wavelengths. This is the geometry that was used in the measurements presented here, with the detail that clouds were observed from far distances so that the view angle range was relatively small. Although Rayleigh scattering, water vapor absorption, and IR emissivity issues are minimized in this case, cloud shadows in the upper views, and the interpretation of the multi-angle distribution in the analysis of a single cloud can still be troublesome. The best geometry for cloud side observations would actually be performed by high altitude aircrafts or satellites, where the platform is completely above the cloud, and side radiances can be observed from the base to the top of the cloud with a single view angle orientation with the sun behind. By definition, this geometry eliminates the possibility of shadows in the observed pixel. Multiangle satellite observations like the ones by MISR (Multi-angle Imaging SpectroRadiometer – (Diner et al.; 1998) have provided some cloud side observations but, unfortunately, MISR lacks the right wavelengths to provide the vertical profile of cloud microphysics and thermodynamic phase explored here.

Figure 3 shows a more appropriate observing geometry using a high altitude aircraft. The main advantage in this case is that the view zenith angle is constant for all portions of the cloud. This geometry advantage allows for better interpretation of the thermal data producing meaningful –dT/dx (where x is the displacement of the aircraft) results clearly separating cloud tops from cloud sides, and providing estimates of the cloud

side (relative) slanted slope. The cloud tops will present the lowest –dT/dx values, as well as the cloud sides with oblique slopes will present lower -dT/dx values than the deep convective columns with nearly vertical slopes on the cloud side. This relative classification of the cloud side slopes is important for the selection of the 3-D look-up-table model to interpret the cloud side radiances. The relative angle between the solar incidence and the cloud side wall is an important factor for the inversion of the droplet effective radius profile, as it will be discussed in the next section. The conceptual plot on the left lower corner of Fig. 3 shows an example of the thermal measurement results for the cloud on the right hand side. The negative slope –dT/dx can be associated with the geometric slope (dz/dx) in the real cloud, relating the thermal IR brightness temperature measurements with the cloud geometry.

2.4 3-D radiative transfer in clouds

It seems natural that an accurate treatment of the cloud side radiances requires the cloud to be treated as a 3-D object. There are several degrees of complexity that can be considered in the 3-D simulation of clouds. For accurate simulations one should account for the cloud vertical structure (variation on cloud droplet or ice crystal size and shape, mixing between ice and water, and variation in water path), shadowing effects, interactions between the cloud sides and the underlying surface, realistic distributions of clouds in a cloud field, and interaction between neighboring clouds. In this study we will use a series of simplifying hypotheses in order to define a simple but still realistic scheme for obtaining detailed microphysical information from the remote sensing of the cloud side spectral radiances. For simplicity, in our quantitative retrievals, we will focus on the illuminated side (directions near the backward scattering) of an isolated convective cloud lying over a dark surface, ignoring the exchange of photons between clouds. A more realist simulation of stochastic cloud fields is performed in the companion paper Marshak et al. (2006). In that paper, several cloud fields with the same stochastic properties as real clouds are generated assuming variable cloud tops, vertical profile of water droplet, mixed phase, and ice particles. Here we compare the results from

Marshak et al. (2006) simulations with our simplified approximations.

In order to build a look-up-table for our quantitative retrievals from the cloud side, rigorous 3-D radiative transfer simulations were performed with the SHDOM (Spherical Harmonics Discrete Ordinate Method – Evans, 1998 and Evans and Marshak, 2005) code for cylindrical clouds consisting of homogenous water droplets, or different types of ice crystal habits (Yang et al., 2000). Individual cylindrical clouds where simulated with effective radii varying between 5–40 μm, optical depths τ_z=50 and 100, and horizontal optical distances varying from τ_x=10 to 100, or optical distance aspect ratios τ_z/τ_x=1, 2, 3, 4 and 5, over dark surface (surface albedo = 0). These simulations included Rayleigh scattering but neglected gaseous absorption. The main purpose of this initial simulation was to compare the extent of the cloud edge effects on the side radiances, and compare results with a traditional plane parallel approximation. For quality assurance, some results from this model were also intercompared with Monte Carlo simulation (Evans and Marshak, 2005) showing good agreement. The SHDOM simulations were performed at 4 wavelengths (0.67, 2.1, 2.25, and 11 μm) with several solar and viewing geometries, in order to produce general look-up-tables for interpreting the cloud side measurements.

Figure 4 shows 2.1 μm reflectance from the side and top of the simplified cylindrical cloud illuminated with 60° solar zenith angle and viewed at 45° viewing zenith angle. Due to the larger absorption by water droplets at 2.1 μm, the side radiances at this wavelength quickly approach an asymptotic behavior after an optical depth of ~30 away from the edge. The lack of absorption at 0.66 μm increases this distance significantly, enhancing the edge effect (see Marshak et al., 2006). This behavior re-affirms that absorbing wavelengths are less sensitive to 3-D effects due to the shorter photon path inside the cloud. For the same reason, a plane parallel approximation works better for clouds at 2.1 μm than at 0.66 μm. Nevertheless, the plane parallel approximation can also be a good approximation to represent cloud side radiances as long as the correct geometry is taken into account. The solar zenith angle and the view zenith angle must be corrected for the appropriate cloud side geometry. The rule of thumb is to use

a vector normal to the studied surface as a geometrical reference and not necessarily the zenith. Therefore to simulate the side reflectance of a cylinder illuminated with solar zenith angle θ_o, and observed from a view zenith angle θ, the plane parallel analogue correspond to a case with θ_{opp}=(90-θ_o) and θ_{pp}=(90-θ). The plane parallel approximation is valid only for modeling cases far away from cloud edges (at least an optical distance 30 from any edge for water droplet r_{eff}=10 μm), over dark surface, where side illumination effects caused by the surface albedo are negligible. Also, the plane parallel approximation for cloud side radiances is valid for effective radii determinations but not necessarily for τ_z or τ_x retrievals. Marhsak et al. (2006) presents more details on this discussion.

The SHDOM simulated cylindrical clouds were used for the generation of retrieval lookup tables to determine the vertical profile of droplet effective radii as a function of the cloud side radiances. For simplicity, the initial retrievals were performed away from cloud edges (avoid the first few pixels near cloud base and top), using look-up-table radiances coming from the center of cylinders with τ_z=100, and aspect ratios τ_z/τ_x = 1, 2, 3, 4 and 5. The validity of the 3-D cylindrical cloud approach used here was studied by producing a 3-D analog of the Nakajima-King diagrams using side reflectances from the center of the cylinders, at λ=0.66 and 2.1 μm as a function of droplet effective radii, and horizontal optical depth τ_x. Figure 5 shows the intercomparison between the Nakajima-King analogs of cylindrical homogeneous clouds versus the stochastic results produced by Marshak et al. (2006). In the later case, the stochastic clouds were composed of complex cloud fields with the 3-D radiative transfer results taking into account shadows and photons traveling between clouds, as well as a complex vertical profile of droplet sizes and thermodynamic phase distribution including, water, mixed phase, and ice. The question to be answered here is the applicability of a simplified cylinder look-up-table in inverting results from such a complex cloud field. Good agreement between the retrieval results obtained from a more sophisticated stochastic cloud model and isolated cylindrical clouds confirms the validity of the later simplified approach, as a first approximation. However, for future applications we propose re-

trievals based on stochastic cloud fields (or other simulated clouds), as in Marshak et al. (2006), which uses a Bayesian approach to provides a distribution of possible effective radii that statistically satisfy to the measured radiances.

2.5 Penetration of the cloud side measurements and the horizontal distribution of the cloud microphysical properties

Cloud side remote sensing produces more information on cases where the vertical profile of cloud droplet (particles) size retrieved near cloud edges can be extrapolated for the whole cloud at a given temperature or height level. Photons at absorbing wavelengths (e.g. 2.1 μm) can only profile a physical volume near the cloud edges. By "near cloud edges" we understand the optical distance a "typical" photon at 2.1–2.3 μm wavelength can penetrate inside the cloud (Platnick, 2000; Marshak and Davis, 2005). Fortunately, the effective radius of cloud droplets is, perhaps, one of the most conservative microphysical property at a given temperature and the same cloud system (Rosenfeld and Lensky, 1998; Freud et al., 2005). Indeed, while both cloud liquid water and droplet concentration vary substantially along a horizontally flying aircraft, the effective radius remains relatively constant (e.g., see Fig. 10 in Rosenfeld and Lensky, 1998 for convective clouds and Figs. 2 and 3 in Blyth and Latham, 2001 for cumulus clouds). In addition to a very comprehensive discussion of this phenomenon given by Freud et al. (2005), we only mention that cloud models (Zev Levin, private communications) also confirm that the assumption of mild fluctuations of the droplet effective radius across the cloud at a given temperature (or at a given height) looks very realistic. Experimental evidences for this fact can be found in Rosenfeld and Woodley (2006b), which shows cross sections of convective elements of severe hailstorms or in their vicinity, where they made aircraft measurements of temperature, hot-wire liquid water content, adjusted FSSP liquid water content, particle number concentrations (2–44 μm in diameter) as measured by the adjusted FSSP, and effective diameter of the FSSP-measured particles. The results show that despite of large variations in liquid water content, the effective diameter of the droplets remain constant across the cloud cross

section. Similar results have been observed by D. Rosenfeld who conducted similar in situ aircraft measurement in convective clouds at widely varying conditions in Brazil, Texas, California, Portugal and Israel. This serves as strong evidence that the droplet effective radius is a conservative property across convective clouds and can effectively be estimated by measurements from the cloud side.

3 Data analysis and results of aircraft measurements

3.1 Vertical profile of effective radius and thermodynamic phase

An example of the new type of cloud side measurements presented in Sect. 2.3 is shown in Fig. 6. This figure shows the results of our first aircraft experiment performed during the CLAIM (Cloud Aerosol Interaction Mission) campaign in Brazil, in January/February 2005, testing the cloud scanner prototype. The central panel shows the actual picture of the cloud under study, while the left panel shows the brightness temperature image overlaid by a temperature profile (white plot) in the center of the cloud. The right panel exemplities the result of our algorithm separating the ice and water components inside the cloud.

The vertical profile of droplet effective radii was inverted using calibrated 2.1 μm reflectances measured on the side of convective clouds during the CLAIM campaign, and the simplified cylindrical 3-D look-up-table described above. Figure 7 (bottom left panel) gives an example of such retrieval showing warm cloud processes near cloud base were droplets grow by diffusion and collision-coalescence, and more efficiently, the mixed phase processes were the droplets grow even faster. The water droplets grew by diffusion and/or collision-coalescence up to about 14 μm effective radius and a temperature of about –11˚C after what the droplets started to freeze and mixed phase processes dominated the particle growth. The mixed phase process took place till a temperature of about –37˚C (respecting the limit of –38˚C for the existence of liquid water) causing the droplets to increase up to 37 μm effective radius. The ice phase

profile shows the particle effective radius decreasing as a function of height. Other cases from the same experiment showed a constant effective radius profile in the ice phase. The droplet size profile shown here and several other results obtained during the CLAIM field campaign are in good agreement with the conceptual models of droplet growth in convective clouds presented by Rosenfeld and Woodley (2003) and Rosenfeld and Lensky (1998) (see Fig. 2). The top panel in Fig. 7 shows a wide angle picture of the cloud under study. Although the cloud morphology in this picture may trick some observers, this cloud is a very deep convective cloud with cloud top temperatures near -90˚C.

A completely independent measurement of the droplet thermodynamic phase is shown in the bottom right panel of Fig. 7. This panel shows the ratio between reflectances at 2.10 μm and 2.25 μm which will be explained later in Sect. 3.2 as an indicator of water, ice, or mixed phase present inside the cloud. It is important to notice that the mixed phase identified in the reflectance ratio 2.10/2.25 μm corresponds unequivocally with the mixed phase droplet growth identified in the effective radius profile. This remarkable agreement once again indicates the power of the cloud side measurements in identifying the cloud microphysical processes inside the cloud. The large amount of information present in this vertical profile substantially increases our understanding of how aerosols may affect clouds and change the precipitation efficiency by driving the droplet growth at the scales where the interaction with the CCN really happens. The vertical profile of effective radius adds very important information on the effect of aerosols on cloud droplets and on the cloud microphysical processes driving the initiation of precipitation. Cloud droplets grow slowly by diffusion of water vapor near the cloud base; then the growth process is dominated by collision-coalescence providing faster droplet growth; the effective radius growth becomes even more efficiently after the beginning of glaciation when the mixed water-ice processes takes over. By the time all the droplets are converted into ice, the particles are significantly larger and the precipitation processes are probably already in effect. Depending on the maturity of the cloud system in study, the vertical profile of the ice portion of the cloud

will show different behaviors as a function of height or cloud temperature. Results may vary from a constant effective radius, as a function of height, to cases where the effective radius may drop significantly above the –38°C isotherm due to homogeneous freezing of small cloud droplets and the nucleation of newly formed ice crystals, on due to precipitation of large ice particles inside the cloud.

Since the freezing temperature depends on the droplet size distribution, which is affected by the aerosol concentration and type, and eventually by the aerosol efficiency to act as ice nuclei, the simple measurement of the cloud thermodynamic phase as a function of the temperature and amount of aerosols can be a good indicator of the interaction between aerosols and clouds.

3.2 Interpretation of the ice-water thermodynamic phase measurements

Platnick (2003 – personal communication) has used two nearby wavelengths around 2.1 μm with the MAS (MODIS Airborne Simulator) for the separation between ice and water in cloud tops. Here we justify the applicability of measurements centered at 2.10 and 2.25 μm for the identification of ice, water, and mixed phase on the vertical profiles measured on the side of convective clouds. Figure 8 illustrates that the primary signal separating ice and water in these wavelengths come from the imaginary component of the refractive index. Ice and water have enough different refractive indices at 2.10 and 2.25 μm that allow us to identify them by simply taking the ratio between the reflectances at these two wavelengths. In addition, we see that the refractive index at these wavelengths is also a weak (but significant) function of the water temperature.

In order to evaluate the power of the ice-water separation algorithm on the vertical profile of complex convective clouds, we used the SHDOM code to simulate radiation reflected from cylindrical clouds with microphysical vertical profile following the conceptual diagrams of Fig. 1. The conceptual diagram used is shown in Fig. 9a illustrating 5 microphysical stages as a function of the temperature or height inside the clouds. Initially the droplets grow by water vapor diffusion, followed by collision-coalescence, a third stage where the droplets have already reached large enough sizes to enable inter-

nal precipitation processes, a mixed phase where ice and water can coexist and further enhance the droplet growth efficiency, and a glaciated stage where all the droplets are frozen. The ice particles were simulated using 5 different ice habits and phase functions proposed by Yang et al. (2000). The Rosenfeld and Woodley (2003) diagrams suggest that at the glaciated stage, the effective radius remain constant as a function of height. Our observations (e.g. Fig. 7 above) show several cases where the particle size at this stage even decreases as a function of height. The cloud side radiances for this model were calculated for 60° solar zenith angle, 50° view zenith angle, and were used to simulate the 2.10/2.25 μm ratio. The results are shown in Fig. 9b, where water droplets show ratio values between 0.78 to 0.9, depending mainly on droplet size effects, and ice particles show ratios between 0.5 and 0.61. It is important to notice that the 2.10/2.25 μm reflectance ratio is also sensitive to different ice crystal habits. The dependence of the 2.10/2.25 μm reflectance ratio on the cloud droplet size and temperature produces some broadening on the final results but, the separation between ice, water, and mixed phase still produces very strong and unambiguous signal.

Experimental measurements of the 2.10/2.25 μm reflectance ratio were performed for several convective clouds (observed during the CLAIM campaign) after separating the water and ice portions of the clouds. Figure 10 shows histograms of the reflectance ratios where the ice values vary from 0.33 to 0.47, and the reflectance ratios for water varied from 0.75 to 0.95. The distribution of ratio values for water agrees well with the simulated values shown in Fig. 9 (above) plus the dependence of the imaginary refractive index with temperature that was presented in Fig. 8. For ice, on the other hand, the experimental values are well below the simulated values, and the differences cannot be explained by the particle size effect alone. This result strongly suggests that the refractive index value for ice shown in Fig. 8 is not correct for the ice clouds measured during this experiment.

In order to show the sensitivity of the reflectance ratio to the imaginary refractive

indices of water and ice at the 2.10 and 2.25 μm, Fig. 10 also shows the ratio:

$$\alpha = \frac{1/m_{i\_2.10\,\mu m}}{1/m_{i\_2.25\,\mu m}}$$

Where m_i=imaginary part of the refractive index at each wavelength. The results for α are shown in the overlaid vertical lines in Fig. 10. Although the refractive index ratio does not equal directly to the reflectance ratio, this comparison shows in simple terms the effect of the spectral refractive indices of water and ice.

4 Suggested satellite observations of cloud side radiances

Following the cloud side measurement concepts describe above, a hypothetical satellite (the 3-D Cloud Aerosol Interaction Mission, or CLAIM-3D) can be proposed with the primary goal of measuring the vertical profile of cloud droplet effective radius, thermodynamic phase, brightness temperature, and its response to the type and amount of aerosol particles surrounding the cloud field. Figure 11 shows a schematic diagram for the CLAIM-3D satellite concept. The cloud side measurements should be composed of enough visible and shortwave infrared measurements to provide effective radius and particle phase retrievals, as well as thermal infrared wavelengths to provide brightness temperature retrievals. Combination between thermodynamic phase and brightness temperature, has key importance in revealing detailed microphysical processes inside the clouds. Multi-angle observations would provide parallax measurements helping even further to reveal details of the cloud structure. Spatial resolution must be small enough to provide profiling information on convective clouds but, due to the general diffuse properties of clouds and the radiative smoothing scale (Marshak et al., 1995), there should be not much benefit of spatial resolutions better than 100 m. Pointing capability is essential to optimize solar illumination and the scattering angle geometry, minimizing shadows and other undesirable 3-D effects. Depending on the time of day,

and the position in the orbit, the optimized observing geometry would call for a forward or backward pointing (along track scanning), or for a geometry pointing side ways off set in the cross track direction (side scanning). As discussed in Sect. 2.3 above, high altitude aircrafts or satellites actually provide the best observation geometry for cloud side measurements allowing for constant view angle observations which further simplifies the retrieval algorithm.

In addition to the cloud side measurements it is essential to provide high quality aerosol retrievals including accurate spectral optical depth and information on size distribution. A comprehensive set of aerosol parameters can be obtained with a combination of multi-angle, wide wavelength range (from UV to 2.3 μm), and polarization measurements. These measurements would provide a comprehensive tool to represent the radiation field and invert detailed and accurate aerosol properties. Although the CCN concentration cannot be directly measured from space, the combination between accurate optical depth and aerosol particle size information can provide important proxies to the concentration and type of CCNs available in a given cloud field. Refractive index measurements can also help in determining aerosol chemical composition and potentially its hygroscopicity properties. Rosenfeld (2006a and 2006b) reviews cloud-mediated impacts of aerosols on Earth's temperature and water resources, and points the role of remote sensing in measuring CCN concentrations and their effect on clouds. Rosenfeld (2006b) pointed out that the multi-angle polarization measurements by the POLDER instrument and the Glory satelitte significantly improve our ability to obtain proxies for CCN aerosols from space, emphasizing particle size as their main characteristic.

The CLAIM-3D mission will build upon the experience of these previous space missions combining comprehensive aerosols and cloud microphysical measurements providing detailed information on how the aerosol particles are affecting cloud microphysics, thermodynamics, and the processes that precede precipitation. The data interpretation would be directly guided by the brightness temperature measurements, and its derivative with respect to the position of the satellite (–dT/dx). This variable, pro-

vides the key to determine if the measured pixel corresponds to cloud top, cloud side, and how stiff are the slopes of the cloud edges. The stochastic/Bayesian approach proposed by Marshak et al. (2006) provides the needed tools to determine the effective radius profile and variance that best fit the measured radiances. The CLAIM-3D concept provides a full set of aerosol and cloud microphysical parameters that significantly improves today's state of the art knowledge on the interactions between aerosol particles and cloud properties.

5 Summary and discussion

The methodology discussed here consists in passively measuring solar radiation photons reflected by the cloud sides to provide the vertical profile of cloud microphysical and thermodynamical properties, as a function of the aerosol type and amount around the cloud field. Cloud side measurements provide a powerful tool to unravel the effect of aerosol particles in changing cloud microphysics, lifetime, dynamics, thermodynamics, and the onset of precipitation. These observations can be performed from ground, aircraft, or satellite, with the best geometry performed with observations from above the clouds, using high altitude aircraft or satellite sensors. The measurements provide:

- a snapshot of the vertical structure of cloud microphysics and thermodynamic phase, as a function of height, or of the brightness temperature profile from the side of the clouds.
- the possibility of obtaining large statistics to allow confident conclusions about the physical processes inside the cloud, and how they are affected by the presence, amount, and type of aerosol particles.

These two conditions cannot be met today by existing remote sensing or in situ capabilities. These results, in conjunction with other measurements of cloud and aerosol characteristics will improve our understanding of the factors influencing cloud development, and the onset and character of precipitation. Results of 3-D radiative transfer

simulations in this work and in the companion Marshak at al. (2006) paper shows the large sensitivity of the cloud side radiances to effective radius, and thermodynamic phase of the cloud particles. We must use this sensitivity to reveal important details of cloud microphysics, and better support the development and validation of cloud modeling activities.

The CLAIM-3D satellite concept proposed here combines several techniques to simultaneously measure the vertical profile of cloud microphysics, thermodynamic phase, brightness temperature, and aerosol amount and type in the neighborhood of the clouds. The wide wavelength range, and the use of mutli-angle polarization measurements proposed for this mission would allow us to estimate the availability and characteristics of aerosol particles acting as cloud condensation nuclei, and their effects on the cloud microphysical structure. These results would provide unprecedented details on the response of cloud droplet microphysics to natural and anthropogenic aerosols in the size scale where the interaction really happens.

Acknowledgements. This work was partially supported by NASA Goddard Space Flight Center New Opportunities Office. We thank J. C. Ceballos, A. Correia, K. Gendreau, K. Longo and G. K. Nishioka for the essential help in collecting the aircraft data, and the CPTEC/INPE support on weather forecast during the CLAIM-2005 campaign in Brazil. We also thank A. Davis, G. Feingold, Z. Levin, B. Mayer, and S. Platnick for the numerous stimulating discussions on this subject.

References

Ackerman, A. S., Toon, O. B., Stevens, D. E., Heymsfield, A. J., Ramanathan, V., and Welton, E. J.: Reduction of tropical cloudiness by soot. Science, 288, 1042–1047, 2000.

Albrecht, B. A.: Aerosols, cloud microphysics, and fractional cloudiness, Science, 245, 1227–1230, 1989.

Andreae, M. O., Rosenfeld, D., Artaxo, P., Costa, A. A., Frank, G. P., and Longo, K. M., Silva-Dias, M. A. F.: Smoking rain clouds over the Amazon, Science, 303, 1337–1342, 2004.

Blyth, A. M. and Latham, J.: A climatological parameterization for cumulus clouds, J. Atmos. Sci., 48, 2367–2371, 2001.

Chang, F.-L. and Li, Z.: Estimating the vertical variation of cloud droplet effective radius using multispectral near-infrared satellite measurements, J. Geophys. Res., 107, 10.10292/2001JD000766, 2002.

Chang, F.-L. and Li, Z.: Retrieving vertical profiles of water-cloud droplet effective radius: Algorithm modification and preliminary application, J Geophys. Res., 108, doi:10.1029/2003JD003906, 2003.

Clothiaux, E. E., Moran, K. P., Martner, B. E., Ackerman, T. P., Mace, G. G., Uttal, T., Mather, J. H., Widener, K. B., Miller, M. A., and Rodriguez, D. J.: The Atmospheric Radiation Measurement Program cloud radars: Operational modes, J. Atmos. Oceanic Technol., 16, 819–827, 1999.

Cotton, W. R.: Atmospheric Thermodynamics and Microphysiscs of Clouds, AT620 Lecture Notes, Summer 2005 revision.

Diner, D. J., Beckert, J. C., Reilly, T. H., Bruegge, C. J., Conel, J. E., Kahn, R., Martonchik, J. V., Ackerman, T. P., Davies, R., Gerstl, S. A. W., Gordon, H. R., Muller, J.-P., Myneni, R., Sellers, R. J., Pinty, B., and M. M.: Multi-angle Imaging SpectroRadiometer (MISR) description and experiment overview. IEEE Trans, Geosci. Rem. Sens., 36(4), 1072–1087, 1998.

Evans, K. F.: The Spherical Harmonics Discrete Ordinate Method for Three-Dimensional Atmospheric Radiative Transfer, J. Atmos. Sci., 55, 429–446, 1998.

Evans K. F. and Marshak, A.: Numerical Methods in Three-Dimensional Radiative Transfer. In: A. Marshak and A.B. Davis, [Eds], "Three-Dimensional Radiative Transfer in Cloudy Atmospheres", Springer, 243–282, 2005.

Freud, E., Rosenfeld, D., Andreae, M. O., Costa, A. A., and Artaxo, P.: Robust relations between CCN and the vertical evolution of cloud drop size distribution in deep convective clouds, Atmos. Chem. Phys. Discuss., 5, 10 155–10 195, 2005.

Frisch, A. S., Fairall, C. W., and Snider, J. B.: Measurement of stratus cloud and drizzle parameters in ASTEX with a Ka-band Doppler radar and a microwave radiometer, J. Atmos. Sci., 52, 2788–2799, 1995.

Hansen, J., Sato, M., and Ruedy, R.: Radiative forcing and climate response, J. Geophys. Res., 102, 6831–6864, 1997.

Holben, B. N., Eck, T. F., Slutsker, I., Tanre, D., Buis, J. P., Setzer, A., Vermote, E., Reagan, J. A., Kaufman, Y. J., Nakajima, T., Lavenu, F., Jankowiak, I., and Smirnov, A.: AERONET – A

federated instrument network and data archive for aerosol characterization, Remote Sens. Environ., 66, 1–16, 1998.

Kaufman, Y. J., Koren, I., Remer, L. A., Rosenfeld, D., and Rudich, Y.: The Effect of Smoke, Dust and Pollution Aerosol on Shallow Cloud Development Over the Atlantic Ocean. Proceedings of the National Academy of Sciences, 102(32), 11 207–11 212, 2005.

Kaufman, Y. J. and Koren, I.: Smoke and Pollution Aerosol Effect on Cloud Cover. SCIENCE, 313, 655–658, doi:10.1126/science.1126232, 2006

Khain A. P., Rosenfeld, D. and Pokrovsky, A.: Simulation of deep convective clouds with sustained supercooled liquid water down to –37.5°C using a spectral microphysics model, Geophys. Res. Lett., 3887–3890, 2001.

Khain, A., Rosenfeld, D., and Pokrovsky, A.: Aerosol impact on the dynamics and microphysics of convective clouds, Q. J. R. Meteorol. Soc., 131, 2639–2663, 2005.

Koren, I., Kaufman, Y. J., Remer, L. A., and Martins, J. V.: Measurement of the Effect of Amazon Smoke on Inhibition of Cloud Formation, Science, 303, 1342–1345, 2004.

Koren, I., Kaufman, Y. J., Rosenfeld, D., Remer, L. A., and Rudich, Y.: Aerosol invigoration and restructuring of Atlantic convective clouds, Geophys. Res. Lett., 32, LI4828, doi:10.1029/2005GL023187, 2005.

Kou, L., Labrie, D., and Chylek, P.: Refractive indices of water and ice in the 0.65- to 2.5um spectral range, Appl. Opt., 32(19), 3531–3540, 1993.

Lensky, I. M. and Rosenfeld, D.: The time-space exchangeability of satellite retrieved relations between cloud top temperature and particle effective radius, Atmos. Chem. Phys., 6, 2887–2894, 2006.

Lohmann, U.: A glaciation indirect aerosol effect caused by soot aerosols, Geophys. Res. Lett., 29, doi:10.1029/2001GL014357, 2002.

Marshak, A., Davis, A., Wiscombe, W., and Cahalan, R. F.: Radiative smoothing in fractal clouds, J. Geophys. Res. (Atmos.), 100, 26 247–26 261, 1995.

Marshak, A. and Davis, A.: Horizontal fluxes and radiative smoothing, in: 3D Radiative Transfer in Cloudy Atmospheres. Springer Berlin Heidelberg, New York, edited by: Marshak, A. and Davis, A., ©2005, 686, ISBN-10 3-540-23958-8 ISBN-13 978-3-540-23958-1, 543–586, 2005.

Marshak, A., Martins, J. V., Zubko, V., and Kaufman, Y. J.: What does reflection from cloud sides tell us about vertical distribution of cloud droplet sizes, Atmos. Chem. Phys., 6, 5295–5305, 2006.

McGraw, R. and Y. Liu: Kinetic Potential and Barrier Crossing: A Model for Warm Cloud Drizzle Formation, Phys. Rev. Lett., 90(1), 01851, 2003.
Nakajima, T. Y. and King, M. D.: Determination of the optical thickness and effective particle radius of clouds from reflected solar radiation measurements – Part I, Theory, J. Atmos. Sci., 47, 1878–1893, 1990.
Nakajima, T., King, M. D., Spinhirne, J. D., and Radke, L. F.: Determination of the optical thickness and effective particle radius of clouds from reflected solar radiation measurements. Part II: Marine stratocumulus observations, J. Atmos. Sci., 48, 728–750, 1991.
Pilewskie, P. and Twomey, S.: Discrimination of ice from water in clouds by optical remote sensing, Atmos. Res., 21, 113–122, 1987a.
Pilewskie, P., and Twomey, S.: Cloud phase discrimination by reflectance measurements near 1.6 and 2.2 mm, J. Atmos. Sci., 44, 3419–3421, 1987b.
Platnick, S.: Vertical photon transport in cloud remote sensing problems, J. Geophys. Res., 105(D18), 22 919–22 935, 2000.
Platnick, S.: Approximations for horizontal transport in cloud remote sensing problems, J. Quant. Spectr. Rad. Trans., 68, 75–99, 2001.
Platnick, S., King, M. D., Ackerman, S. A., Menzel, W. P., Baum, B. A., Riedi, J. C., and Frey, R. A.: The MODIS cloud products: Algorithms and examples from Terra. IEEE Trans, Geosci. Remote Sens., 41(2), 459–473, 2003.
Rosenfeld, D.: TRMM observed first direct evidence of smoke from forest fires inhibiting rainfall, Geophys. Res. Lett., 26, 3105–3108, 1999.
Rosenfeld, D.: Suppression of rain and snow by urban and industrial air pollution, Science, 287, 1793–1796, 2000.
Rosenfeld, D., and Lensky, I. M.: Spaceborne sensed insights into precipitation formation processes in continental and maritime clouds, Bull. Amer. Meteorol. Soc., 79, 2457–2476, 1998.
Rosenfeld D. and Woodley, W. L.: Deep Convective Clouds with Sustained Supercooled Liquid Water Down to –37.5°C, Nature, 405, 440–442, 2000.
Rosenfeld D. and Ulbrich, C. W.: Cloud microphysical properties, processes, and rainfall estimation opportunities. Chapter 10 of "Radar and Atmospheric Science: A Collection of Essays in Honor of David Atlas", edited by: Wakimoto, R. M. and Srivastava, R., Meteorological Monographs, 52, 237–258, AMS, 2003.
Rosenfeld, D., and Woodley, W. L.: Closing the 50-year circle: From cloud seeding to space and back to climate change through precipitation physics. Chapter 6 of "Cloud Systems,

Hurricanes, and the Tropical Rainfall Measuring Mission (TRMM)", edited by: Tao, W.-K. and Adler, R. F., 234pp., 59–80, Meteorol. Monogr. 51, AMS, 2003.
Rosenfeld D.: Aerosol-Cloud Interactions Control of Earth Radiation and Latent Heat Release, Space Sci. Rev., 9p., doi:10.1007/s11214-006-9053-6, 2006a.
Rosenfeld D: Aerosols, Clouds, and Climate, Science, 312, 1323–1324, 2006b.
Rosenfeld, D., Kaufman, Y., and Koren, I.: Switching cloud cover and dynamical regimes from open to closed Benard cells in response to aerosols suppressing precipitation, Atmos. Chem. Phys., 6, 2503–2511, 2006a.
Rosenfeld, D., Woodley, W. L., Krauss, T. W., Makitov, V.: The Structure of Severe Convective Storms in Mendoza, Argentina. J. Appl. Meteorol., 45, 1261–1281, 2006b.
Twomey, S.: The influence of pollution on the shortwave albedo of clouds, J. Atmos. Sci., 34, 1149–1152, 1977.
Williams, E., Rosenfeld, D., Madden, M., et al.: Contrasting convective regimes over the Amazon: Implications for cloud electrification, J. Geophys. Res., 107(D20), 8082, doi:10.1029/2001JD000380, 2002.
Yang, P., Liou, K. N., Wyser, K., and Mitchell, D.: Parameterization of the scattering and absorption properties of individual ice crystals, J. Geophys. Res., 105, 4699–4718, 2000.

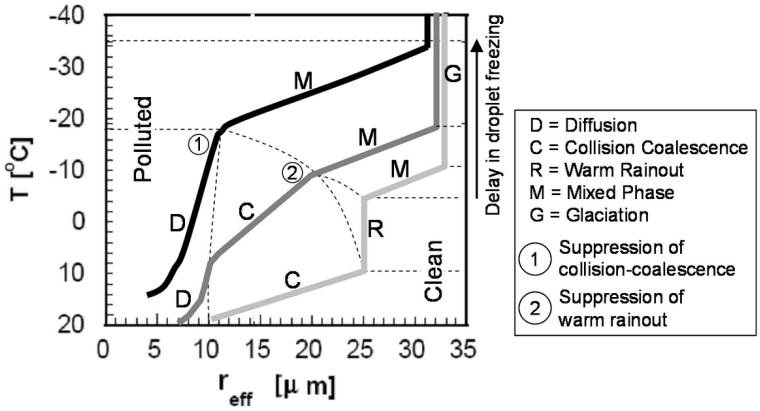

Fig. 1. Conceptual diagram adapted from Rosenfeld and Woodley (2003), describing 5 microphysical stages (droplet growth by diffusion, collision-coalescence, warm rainout, ice-water mixed phase, and glaciated phase) common to deep convective clouds and their response to the concentration of pollution aerosols. The bottom curve shows the case of maritime environment with low CCN concentration and the possibility of warm rain processes; the middle curve corresponds to commonly found continental cases, where the larger number of CCN aerosols helps to suppress warm rain process and glaciation starts at slightly lower temperatures; the top curve represents extremely polluted cases where the very large number of CCNs produce smaller and more numerous droplets at cloud base suppressing the beginning of collision-coalescence processes, and postponing the start of droplet freezing to much lower temperatures. Intermediate situations to the above curves are also possible.

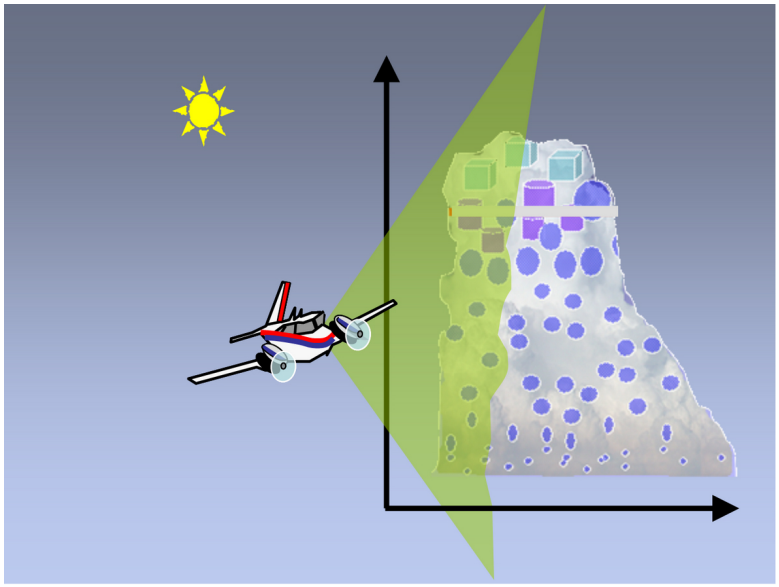

Fig. 2. Cloud side observations from low altitude aircraft.

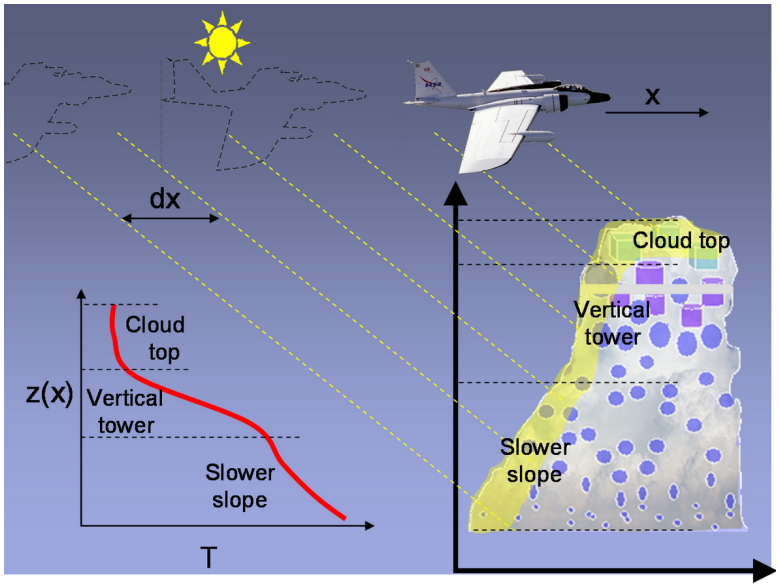

Fig. 3. Schematic representation of cloud side measurements performed form high altitude aircraft or satellite. In this geometry, the cloud is always observed from a single view angle perspective and different altitudes of the cloud are observed by moving the aircraft rather than employing a moving scan mirror. The geometry can always be optimized to reduce shadows and other issues. The insert in the lower left corner shows an idealized measure of temperature as a function of height of the cloud to the right. The more vertical the cloud wall, the more quickly the temperature changes with height. Cloud tops display almost constant temperature with the satellite displacement. The expression "slower slope" in the figure refers to regions where the cloud wall is not vertical, producing slower changes in temperature as a function of cloud height.

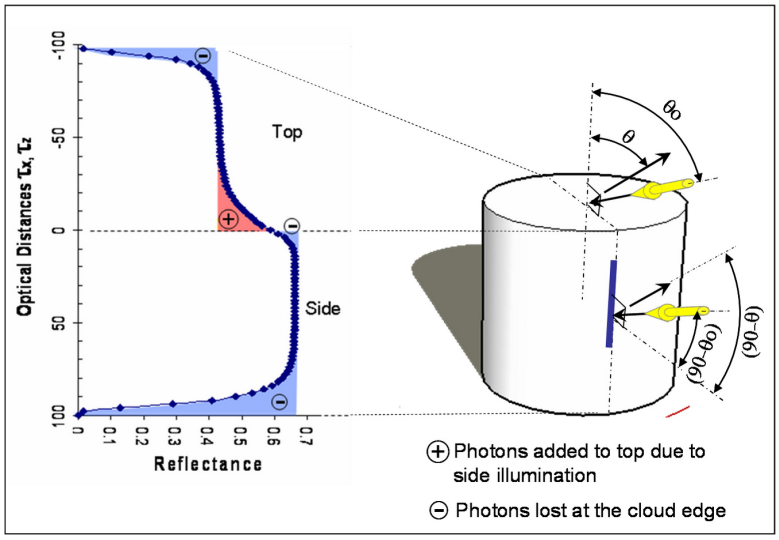

Fig. 4. Cloud side and top radiances at 2.1 μm calculated with the 3-D radiative transfer code SHDOM for a simplified cylindrical cloud with homogeneous r_{eff}=10 μm water droplets, solar zenith angle θ_o=60°, and view zenith angle θ=45°. The colored (blue and red) areas around the plot represent photons been added or lost near the cloud edges. In this particular case the top reflectance is lower than the side reflectance due to the relative angle between the solar illumination and a vector normal to the side or the top surfaces. The relative angle with the top surface vector is 60° whereas the angle with the side vector is 30°. The blue line along the surface of the cylinder represents the region where there is saturation and the 2.1 μm reflectance from the cylinder equals a plane parallel result with the proper geometry. A point half way along the blue line represents the general place that was selected to construct our 3-D look-up-table from retrievals away from the cloud edges. Other regions of the cylinder could be used for retrievals closer to cloud base or top.

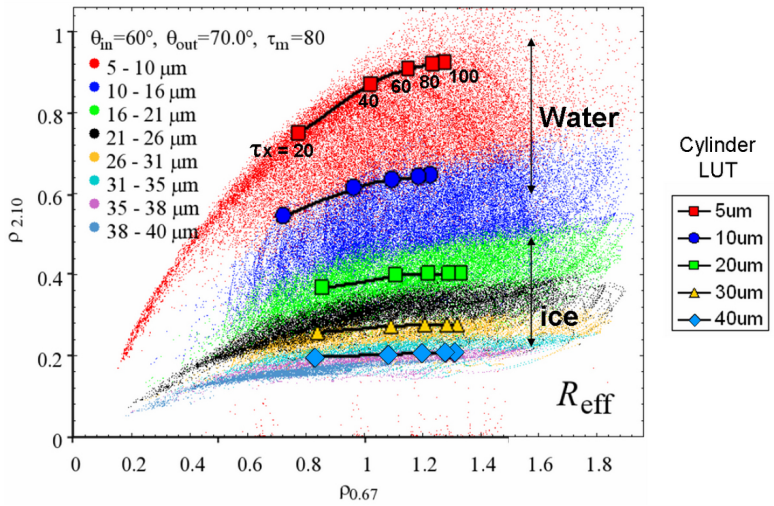

Fig. 5. The collection of colored dots in the background represent the 3-D analog of the plane parallel Nakajima-King type of diagrams for stochastic cloud fields and a variable vertical profile of droplet effective radii, and thermodynamic phase. The overlaid black lines and markers were calculated by individual homogeneous cloud cylinders with total τ_z=100, effective radius as showed in the legend, and optical distance aspect ratios of 5, 4, 3, 2, and 1. A combination of ice and water particles were used in both simulations for the cylindrical and for the stochastic cloud fields.

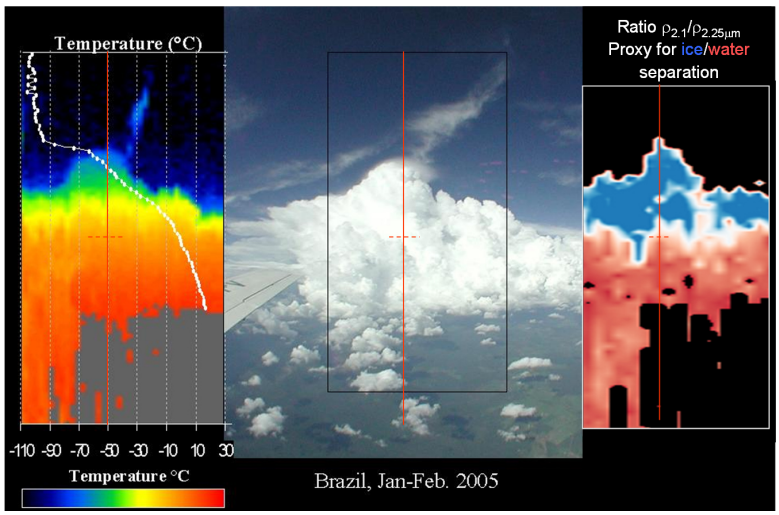

Fig. 6. Cloud side measurements performed with the cloud scanner prototype. The left panel shows the brightness temperature profile, the center panel shows the actual picture of the cloud being observed, and the right panel shows and image of the ratio of reflectances at 2.10/2.25 μm, which represents the separation between ice and water particles in the cloud. The white line and dots on the left panel represents the temperature profile that was measured over the solid red line in the center of the image. The same solid red line is shown on the center and right panels of the figure. The red dashed horizontal line represents the zero Celsius mark.

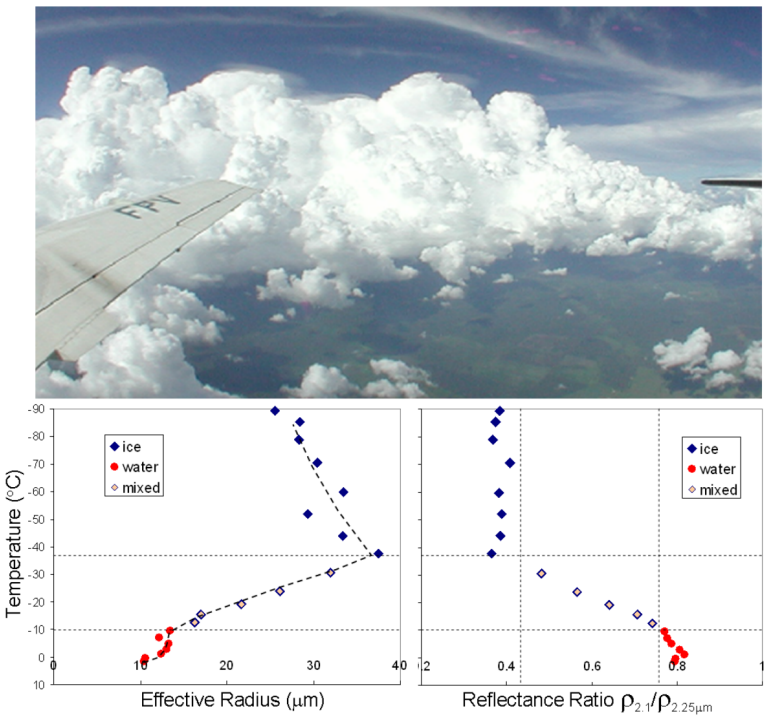

Fig. 7. Effective radius retrieved with radiances from the cloud side (bottom left plot) and separation between ice and water determined by the ratio between reflectances 2.10/2.25 μm (bottom right plot) as a function of the cloud temperature profile. The top image represents a wide field picture of the cloud system under study.

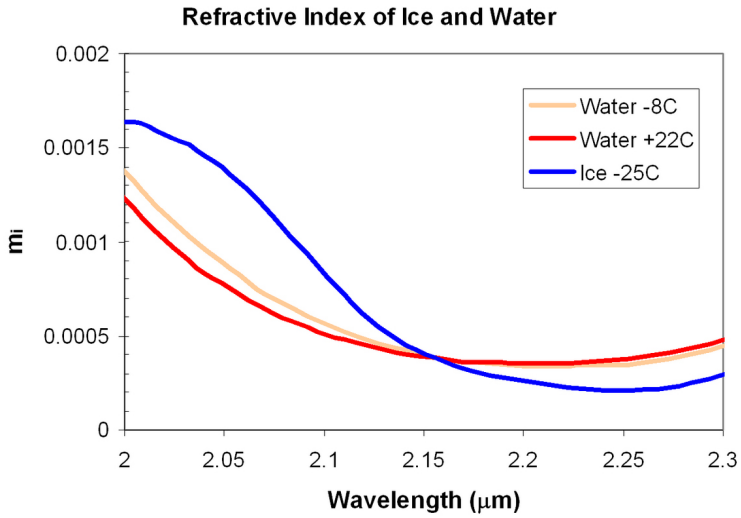

Fig. 8. Data extracted from Kou et al. (1993) shows the spectral dependence of the imaginary component of the refractive indices of ice and water between 2.0 and 2.3 μm, showing the crossing point around 2.15 μm. The water case also shows some dependence with temperature.

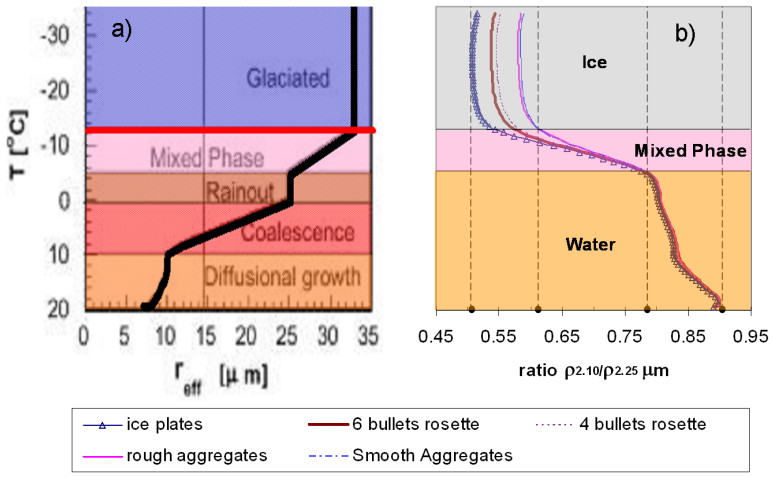

Fig. 9. Panel **(a)**: adapted from Rosenfeld and Woodley (2003 – Fig. 1) shows the "the general case" effective radius and thermodynamic profile used here for the SHDOM simulation. Panel **(b)**: SHDOM simulation of the reflectance ratios (2.10/2.25 μm) based on a cylindrical cloud with panel (a) profile of particle effective radii and thermodynamic phase showing the sensitivity of this ratio to the presence of water, ice, and mixed phase.

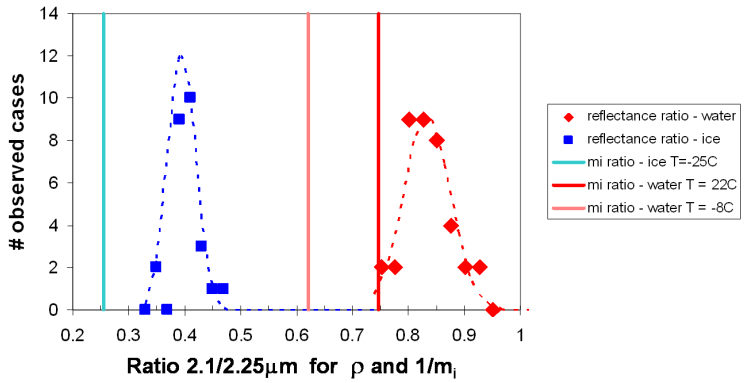

Fig. 10. Histograms of experimental measurements of the reflectance ratio $\rho_{2.10}/\rho_{2.25\,\mu m}$ for ice and water clouds. The red dots show results for the water portion of convective clouds and the blue dots for the ice component. The vertical lines show ratios of the $(1/m_i)$ factor for the same wavelength ratio, where m_i is the imaginary component of the refractive indices of water (red colors for 2 different temperatures) and ice (blue).

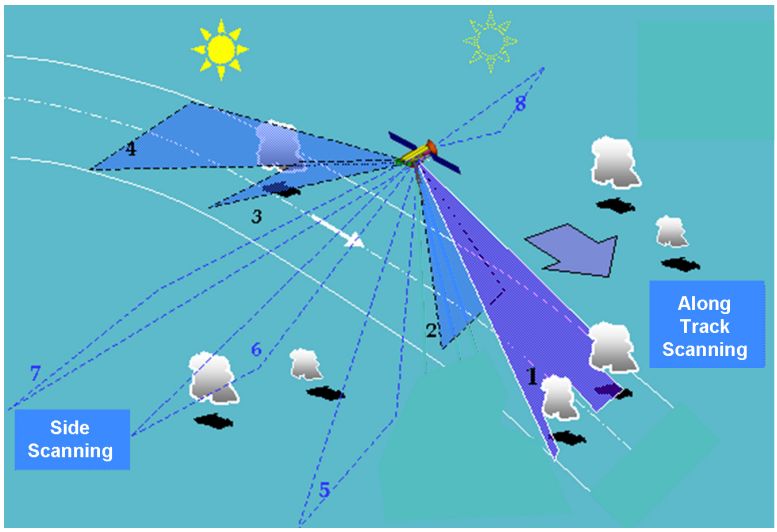

Fig. 11. Conceptual design of a 3-D Cloud Aerosol Interaction Mission satellite (CLAIM-3D) specially designed to perform detailed measurements of aerosols particles and its influences on cloud microphysical properties and on the onset of precipitation. The along track or the side scanning geometries should be optimized according to the time of the day, and relative position of the sun in the satellite orbit. The different numbered viewing geometries in the figure correspond to examples of multi-angle observations for detailed aerosol retrievals, and cloud parallax observations.